Ass. Univ. Bull. Environ. Res. Vol. 10 No. 1, March 2007

AUCES

NUMERICAL SIMULATION AND EXPERIMENTAL STUDY ON STACK-GAS DISPERSION EMITTED FROM DIFFERENT ELEVATED POINT SOURCE IN AN URBAN ENVIRONMENT

Mohamed F. Yassin

Dept. of Mining & Met. Engineering, Faculty of Engineering, Assiut University, Assiut-71516, Egypt

E-mail: mfy_64@yahoo.com/mfy@aun.edu.eg

ABSTRACT:

The flow and dispersion of stack-gas emitted from different an elevated point source around flow obstacles in an urban environment have been investigated theoretically using computational fluid dynamics models (CFD) and experimentally in the diffusion wind tunnel under different condition of thermal stability using a tracer gas technique without buoyancy. The flow and dispersion fields in the boundary layer in an urban environment were examined at different flow obstacle. Gaseous pollutant is discharged in the simulated boundary layer over the flat area. The CFD models used for the simulation were based on the steady-state Reynolds-Average Navier-Stoke equations (RANS) with κ-ε turbulence models; standard κ-ε and RNG κ-ε models. The flow and dispersion data measured in the wind tunnel experiments were compared with the results of the CFD models in order to evaluate the prediction accuracy of the pollutant dispersion. The results of the CFD models wind tunnel experiments showed good agreement with the results of the wind tunnel experiments. The obtained results indicate that the turbulent velocity is reduced by the obstacles models, and the maximum dispersion appears around the wake region of the obstacles. Moreover, these results are used to validate the corresponding Gaussian dispersion model prediction.

INTRODUCTION:

The dispersion of potentially hazardous pollutants emitted from an elevated point source such as stack-gas is of great concern when addressing the possible consequence of such releases on the health and safety of people and environment in the vicinity of the stack. Many variables affect the emission dispersion from stack such wind speed and direction, atmospheric stability, stack height, surrounding buildings, trees and topography, stack exhaust velocity and initial pollutant concentrations. There is no doubt that the ground-level concentration of a pollutant near-source can be reduced by increasing the height at which the pollutant is released to the atmosphere. However, from a practical standpoint the benefits in lower concentration must be balanced against the increased cost incurred in construction taller stacks.

A series of wind tunnel experiments and numerical simulations have been performed with the aims of simulating present conditions and understanding the phenomenon of air pollution diffusion emitted from the elevated point source. For instance, wind tunnel experiments have also been performed for flow

around a cube and prismatic obstacles and the variations of flow with obstacle dimensions have been compared with those under a flat-plate condition, also including the stack gas diffusion (e.g. Wilson, D.; 1979, Schulman and Scire, J.; 1991, Wilson, D.J. and Lamb, B.; 1994, Meroney, *et al*.; 1999), have been made. In an examination of the flow and concentration behind a model cube in the wind tunnel, Merony and Yang (1971) and other varied Vs/U, Hs/H and wind direction. There have also been a number of wind tunnel studies of flow and/or dispersion around a single surface- mounted obstacles and small group of building in a turbulent boundary layer of Snyder, 1993, Snyder, Lawson, 1994, and others. For instance, the numerical simulation of the flow and prediction of pollutant dispersion around obstacles buildings have been carried out by many authors using physical simulation such as in Halitsky (1963), Robins and Castro (1977), Wilson and Britter (1982), Wen-Whai and Meroney (1983), Huber (1989), Isaacson and sandri (1990), Higson *et al.* (1994), Saathoff *et al.* (1995), Macdonald *et al.* (1998), Mavroidis and Griffiths (2001), and Mfula *et al* (2005).

The main objective of the current study is to conduct a wind tunnel investigations with CFD simulation to improve our understanding and computational modeling of the flow and pollutant dispersion emitted from an elevated point source around flow obstacles in an urban area under different types of atmospheric stability within the atmospheric boundary layer. Moreover, Sufficient data to validate the corresponding Gaussian dispersion model prediction are obtained. The flow and diffusion fields in the boundary layer in an urban environment were examined in three flow obstacle cases: (a) without flow obstacles, (b) after 2-D plate model obstacle, and (c) after 3-D cubic obstacle model. Commercial Computational Fluid Dynamics, CFD software, such as FLUENT (2005) solves conservation equations for continuity, momentum, energy and concentration.

EXPERIMENTAL SET-UP:

Closed thermal diffusion wind tunnel was used to perform the experiment. The schematic diagram of the experimental set-up in the present study is illustrated in Fig. (1). Three different types of thermal stratification (stable, neutral and unstable) within the atmospheric boundary layer were created in the test section by controlling the inflow temperature and wind tunnel floor temperature. Heating the air and cooling the wind tunnel floor produced a stable stratified layer. The inflow temperature (T_i) and wind tunnel floor temperature (T_f) were set at 27.8°C and 21.0°C respectively, where the Bulk Richardson number ($Ri_B=gH\ (T_i-T_f)/T_w\ U^2$) was set at 0.04 and Reynolds number (R_e) was 6×10^3. While, cooling the air and heating the wind tunnel floor produced an unstable stratified layer. The wind temperature and wind tunnel floor temperature were 11.9 and 16.0°C respectively, where Ri_B was at –0.06 and R_e was 10×10^3. In neutral stratified layer, Ri_B was 0.0 and R_e was 4×10^3. The scale of the model was also set to be 1:500. The obstacle two-dimensional plate was 60 mm height and 1600 mm width. The obstacle three-dimensional cubic building model was 60×60×60 mm. The stack is modeled by the cylinder with inner and outer diameter of 4 & 6 mm. The schematic diagrams of flow obstacles and different elevated stack model are illustrated in Fig. (2). The model stack was located at X=0. Measurements were made with

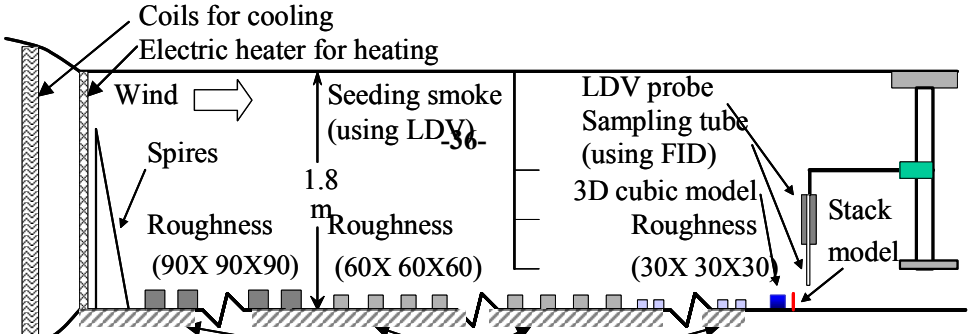

Fig. (1): Experimental set-up in wind tunnel

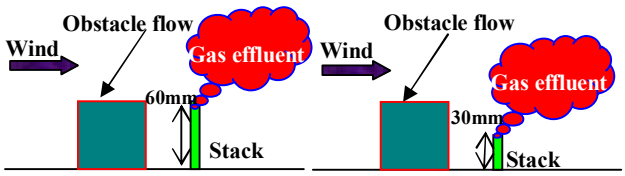

Fig. (2): Flow obstacles and different elevated point source

the model stack height of 60 mm and changed to 30 mm with three different atmospheric conditions to clarify the effect of source height on diffusion.

A Laser Doppler Anemometer, LDA was used to measure the mean velocities and turbulence intensities in longitudinal and vertical directions. The flow and floor temperatures were measured using thermo-couple with copper-constantan thermocouples, which is installed at five positions.

Ethylene, C_2H_4, was used as tracer gas and released from a point source for diffusion measurements. A hydrocarbon analyzer detector (FID) was used to measure the C_2H_4 concentration. The concentration measurements, are presented in the ratio of C/C_o, where C is the measured concentration, and C_o is the reference concentrations ($C_o=Q/U_HH_H^2$, where Q is the source volume flow rate, U_H is the free stream velocity at the height of obstacle, H_H). In the present study, the emission velocity from the stack was 10% of the free stream velocity. Therefore, the effluent velocity of the pollutant is assumed negligible. Since a density of C_2H_4 gas is almost the same as, the density of pollutant gas can be thought to have the same density at the height of the pollutant effluent in the boundary layer.

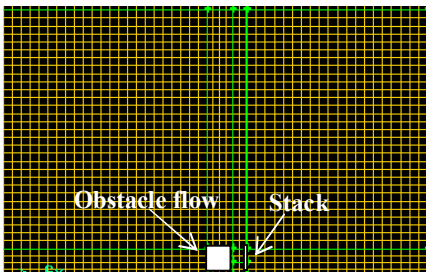

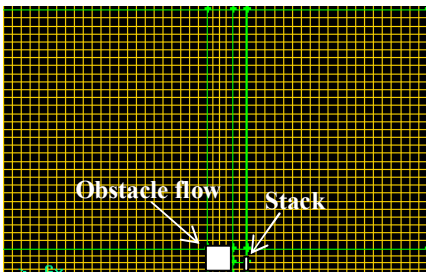

Fig. (3): Computational domain and mesh division

EXPERIMENTAL CONDITIONS:

All these experiments were carried out with the following conditions: a) wind velocity profile of ¼ power law is simulated for all three cases, b) gaseous pollutant is discharged in the simulated boundary layer over the flat area, c) the effluent velocity of the pollutant is set to be negligible, d) the density of pollutant gas is the same as the height of the pollutant effluent in the boundary layer and e) the stratified wind tunnel experiments were performed under three atmospheric conditions: stable (Ri_B=0.04), neutral (Ri_B=0) and unstable (Ri_B=-0.06).

κ-ε TURBULENCE MODELS:

1-Geometrical Configuration

The computational mesh employed was a conventional non uniform mesh for which the number of grid cells, faces and nodes were 345360 cells, 1020957 faces, and 360696 nodes. A typical grid configuration in the near wake region of the building model is shown in Figure (3). The final meshes consist of fluid cell. All calculations were performed using FLUENT 6.2.16, a commercial finite volume –based CFD model (FLUENT, 2005). In addition, the geometry was modeled using GAMBIT 2.2.30 software.

2-Governing Equation:

The fluid flow was modeled by partial differential equations describing the conservation of mass, momentum and species concentration in three rectangular Cartesian coordinate directions for steady, incompressible flow which after Reynolds averaging become:

Continuity equation:

$$\frac{\partial u_i}{\partial x_i} = 0 \quad \textbf{(1)}$$

Momentum equation:

$$\frac{\partial u_i}{\partial t} + \frac{\partial}{\partial x_j}(u_j u_i) = -\frac{1}{\rho}\frac{\partial p}{\partial x_i} + \frac{\partial}{\partial x_j}\left\{\nu\left(\frac{\partial u_i}{\partial x_j} + \frac{\partial u_j}{\partial x_i}\right) - \overline{u_i' u_j'}\right\} \quad \textbf{(2)}$$

Species transport equation:

$$\frac{\partial c}{\partial t}+\frac{\partial u_j c}{\partial x_j}=\frac{\partial}{\partial x_j}\left(D\frac{\partial c}{\partial x_j}-\overline{c'u'_j}\right)+S_c \quad \textbf{(3)}$$

The Reynolds stress and turbulent flux in equations (2) and (3) are parameterized in terms of grid-resolvable variables as

$$-\overline{u'_i u'_j}=\nu_t\left(\frac{\partial u_i}{\partial x_j}+\frac{\partial u_j}{\partial u_i}\right)-\frac{2}{3}T_{KE}\delta_{ij} \quad \textbf{(4)}$$

$$-\overline{c'u'_j}=\nu_c\frac{\partial c}{\partial x_j} \quad \textbf{(5)}$$

$$\nu_t=c_\mu\frac{T_{KE}^2}{\varepsilon} \quad \textbf{(6)}$$

where v_t and v_c are the turbulent viscosities of momentum and pollutant concentration, respectively, δij is the kronecker delta, T_{KE} is the turbulent kinetic energy.

Turbulent energy transport equation.

$$\frac{\partial T_{KE}}{\partial t}+\frac{\partial T_{KE}u_i}{\partial x_i}=\frac{\partial}{\partial x_i}\left(\frac{\nu_t}{\sigma_k}\frac{\partial T_{KE}}{\partial x_i}\right)+\nu_t\left(\frac{\partial u_i}{\partial x_j}+\frac{\partial u_j}{\partial x_i}\right)\frac{\partial u_i}{\partial x_j}-\varepsilon \quad \textbf{(7)}$$

To model the turbulent dissipation rate, the standard κ-ε model (Launder, 1974) and RNG κ-ε model (Yakhot, 1992) are adopted here for computational efficiency and accuracy. The RNG κ-ε model differs from the standard κ-ε turbulence scheme only through the modified equation for ε, which includes an additional sink term in the turbulence dissipation equation to account for non-equilibrium strain rates and employs different values for the model coefficients (Kim *et al.*, 2004). The turbulent dissipation rate in the standard κ-ε model expressed by the following equation:

$$\frac{\partial \varepsilon}{\partial t}+\frac{\partial \varepsilon u_i}{\partial x_i}=\frac{\partial}{\partial x_i}\left(\frac{\nu_t}{\sigma_\varepsilon}\frac{\partial \varepsilon}{\partial x_i}\right)+c_{1\varepsilon}\frac{\varepsilon}{T_{KE}}\nu_t\left(\frac{\partial u_i}{\partial x_j}+\frac{\partial u_j}{\partial x_i}\right)\frac{\partial u_i}{\partial x_j}-c_{2\varepsilon}\frac{\varepsilon^2}{T_{KE}} \quad \textbf{(8)}$$

On other hand, the turbulent dissipation rate in the RNG κ-ε model expressed by the following equation:

$$\frac{\partial \varepsilon}{\partial t}+\frac{\partial \varepsilon u_i}{\partial x_i}=\frac{\partial}{\partial x_i}\left(\frac{\nu_t}{\sigma_\varepsilon}\frac{\partial \varepsilon}{\partial x_i}\right)+c_{ls}\frac{\varepsilon}{T_{KE}}\nu_t\left(\frac{\partial u_i}{\partial x_j}+\frac{\partial u_j}{\partial x_i}\right)\frac{\partial u_i}{\partial x_j}-c_{2\varepsilon}\frac{\varepsilon^2}{T_{KE}}-R \quad \textbf{(9)}$$

where σ_k, σ_ε, $c_{\varepsilon 1}$ and $c_{\varepsilon 2}$ are empirical constants. An extra last term on right-hand side of equation (9) is an extra strain rate given by

$$R = c_\mu \eta^3 \varepsilon^2 \frac{1-\eta/\eta_0}{k(1+\beta_0 \eta^3)} \quad \textbf{(10)}$$

$$\eta = \frac{T_{ke}}{\varepsilon}\left\{\left(\frac{\partial u_i}{\partial x_j}+\frac{\partial u_j}{\partial x_i}\right)\frac{\partial u_i}{\partial x_j}\right\}^{1/2} \quad \textbf{(11)}$$

where, u_i is the ith mean component; p is the deviation of pressure from its reference value; c is the mean concentration of any passive scalar (say, any pollutant); u`and $c$` are fluctuations from their respectively u_i and c, respectively and ρ is the air density. T_{KE} and ε stand for the turbulence kinetic energy and its rate of dissipation, respectively. v is the kinematic viscosity of air, D is the molecular diffusivity of pollutant, S_c denotes the source of pollutant. c_μ, σ_k, σ_ε, $c_{1\varepsilon}$, $c_{2\varepsilon}$, c_2, σ_c, η_0 and β are the turbulence model constants tabulated in Table (1).

In modeling urban flow and dispersion, smaller grid size is desirable around building model to better resolve flow and dispersion field there. To make the CFD model efficient for a given computing resource, a non-uniform grid system is implemented in the model. The above governing equations are solved numerically on a staggered grid system using a finite-volume method with the semi-implicit method for pressure-linked equation (SIMPLE) algorithm (Patanker, 1980). For further details of the numerical procedure, refer Baik *et al.* (2003).

3-Boundary Conditions:

A wall function was employed in the near-wall region. The inlet velocity profile for the atmospheric boundary layer was applied based on wind profile through the wind tunnel experimental data as shown in Fig. (4). The inlet profiles for the turbulence kinetic energy T_{KE} and dissipation rate ε are found in FLUENT and read.

$$T_{KE} = \frac{u_\tau^2}{\sqrt{c_\mu}} \quad \textbf{(13)}$$

$$\varepsilon = \frac{c_\mu^{3/4}(T_{Ke}^{3/2})}{l} \quad \textbf{(14)}$$

where u_t is the friction velocity and l is the turbulence length scale. More details about equations (13) and (14) refer to FULENT (2005).

Table (1): Turbulence model constant values

Model	Constant	c_μ	σ_k	σ_ε	$c_{1\varepsilon}$	$c_{2\varepsilon}$	c_2	σ_c	η_0	β
Standard	Value	0.09	1.0	1.3	1.44	1.92	-	0.7	-	-
RNG		0.0845	0.1719	0.1719	1.42	1.68	1.68	-	4.38	0.012

RESULTS AND DISCUSSION:

1-Simulated boundary layer:

A simulated atmospheric boundary layer was obtained by using a combination of spires and roughness elements on the floor of the tunnel as shown in the schematic diagram of Fig.(4). This combination of spires and roughness elements produced a simulated atmospheric boundary layer with a normal depth, δ, of 1000 mm and a free stream wind speed, U_∞ of 1.3 ms^{-1}. Fig. (4) shows the simulated turbulent boundary layer in the wind tunnel under three atmospheric conditions: stable, neutral and unstable at X/H_{600}=-3 (X/H_{600}=0.0 and -0.05 corresponding to the position of the model stack and the flow obstacles). Fig. (5) shows typical temperature profiles in the vertical direction for stable and unstable stratified boundary layer at X/H_{600}=-3, 0, 0.7, 1 and 1.3. On the stable stratified flows, show almost linear profiles in the vertical direction and uniform temperature profiles at the stream-wise direction.

2-Flow characteristics of the boundary layer:

The flow profiles were made at three different spots along the centerline of the wind tunnel; X/H_{600}=0, 0.2, and 0.6. The flow obstacles were located at X/H_{600}=-0.05. All the velocity data are non-dimensionalized by the reference velocity U_{600} at the height of 600 mm. All the vertical profiles were measured in the turbulent boundary layer starting at 3 mm above the floor. The CFD and wind tunnel results in the flow patterns for all three atmospheric conditions; neutral, stable and unstable cases with three flow obstacle cases are shown in Figs. (6 to 11). As shown in these figures, agreement between the CFD and wind tunnel results for flow characteristics is quite good under thermal stability. The difference was without obstacle and with cube model under unstable condition. The buoyancy forces affect the mean stream-wise and turbulence in the region up to $Z/H_{600}\leq 2$. A thick internal boundary layer can be seen in the case with plate obstacle due to increased turbulence velocity in the three atmospheric conditions, while in the case with cube obstacle, the internal boundary layer generated is thin and more or less the same in the case without obstacles. The reattachment length of the separated flows with plate obstacle is longer than that with the cubic model. The profiles of mean velocity in the leeward direction with the three flow obstacle cases in the neutral and stable boundary layer thickness are approximately the same, but the mean velocity profiles are increased in the unstable boundary layer due to increase in the turbulence, which augments momentum transfer from higher to lower levels. The value of turbulence velocity in the leeward with the plate model is higher than that without obstacles and with the cube model.

3-Dispersion characteristics of the boundary layer:

To establish dispersion characteristics of the simulated boundary layer, dispersion concentration were predicted using CFD models and wind tunnel experiment through the atmospheric stability with the three flow obstacle at three leeward distances: X/H_{600}=0.2, 0.3, and 0.6. The model of the stack (H_s) was located at X/H_{600}=0. Concentration predication were made using the model stack height of H_s/H=1 and changed to 0.5 for the same three cases, where, H is a height of obstacle model. The dispersion concentration, K were measured in the boundary layer at stack height, H_s/H=1

and 0.5 for all three atmospheric conditions with the three flow obstacle cases are shown in Figs. (12 to 17). In general, when effluents come out of the vertical stack at low momentum or low mean vertical velocity, and horizontal flow sufficiently strong around the stack, the effluent plume may be drawn down in the low pressure region in the near wake of the stack. This phenomenon is referred as stack downwash (Arya, 1999). In these figures, the CFD simulation predicted a similar concentration diffusion with that in wind tunnel experimental results. The computed concentration diffusion using the standard κ-ε model was observed quite agreement with the experimental results. The discrepancies in the spread concentrations between the wind tunnel and CFD models at some points in the vertical profiles may be due to low Reynolds number in the wind tunnel. The peak value of concentration for the three atmospheric conditions with the three cases of flow obstacle are ranging from 4 to 9 at a half stack height, where the effluent is emitted near the separation-reattachment region and created the downwash due to the emission velocity from the stack was 10% of the free stream velocity. Dispersion concentration using the plate model is less than that of the cubic model due to the increased turbulence velocity for the plate model. While, at the half stack height, the concentration without flow obstacle is higher than that with the plate and cube model. The value of concentration when using the plate model in the three atmospheric conditions is approximately the same at H_s/H=0.5 and 1, this is also found in the case of the cube model. But, the value of concentration without obstacle at H_s/H=0.5 is higher than that of H_s/H=1 because of the increased stream velocity. The maximum concentration is found around the wake region of the obstacles. Therefore, the spread concentration is high near the stack and getting smaller as the distance increased away from the stack. In general, the spread concentration for the unstable is higher than that of the neutral and stable atmospheric conditions (Ogawa, 1974) as drawn also the present work, the concentration in an unstable case is higher than that in neutral and stable cases in the case of H_s/H=0.5 and 1. This is due to the decrease of turbulent diffusion in unstable condition.

CONCLUSIONS:

After the careful investigation on the flow and pollutant diffusion in an urban environment using CFD models and wind tunnel experiments, the results obtained may be summarized as the following: (1) The buoyancy forces have effect on mean stream-wise and turbulence in the region up to $Z/H_{600} \leq 2$, (2) A thick internal boundary layer is generated in the case with plate model, (3) The inner boundary layer is very thick around the wake region due to the turbulence mixing, (4) The peak concentrations for the three atmospheric conditions with the three flow obstacle cases are ranging from 4 to 9 at the half stack height, (5) Dispersion concentration in unstable case is higher than that in neutral and stable cases, (6) Dispersion concentration for the cubic model are higher than that of the plate model, (7) The value of concentration with stack height Hs/H=0.5 is higher than that when Hs/H=1, and (8) The maximum concentration is found around the wake region of the obstacles.

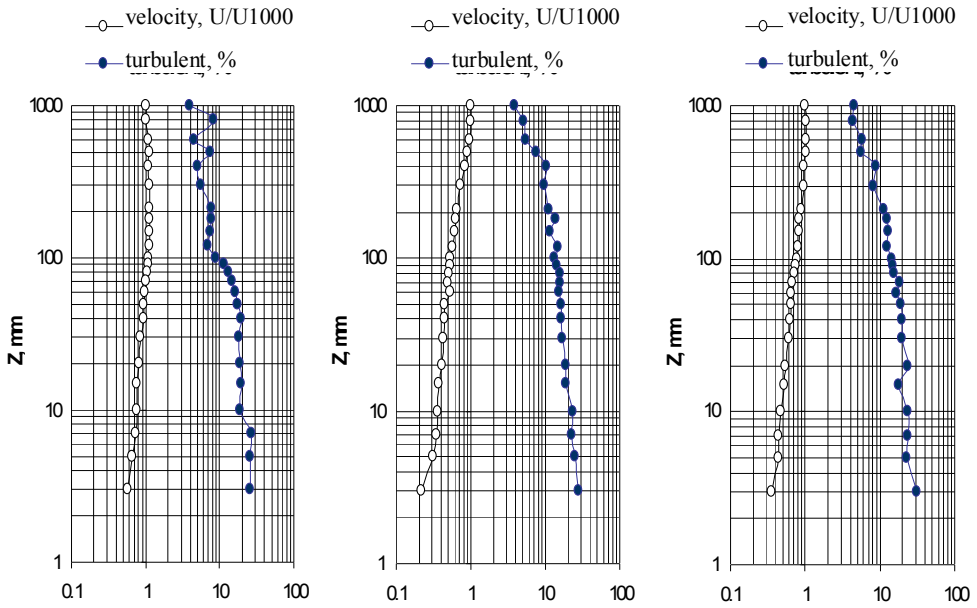

(1) neutral (2) stable (3) unstable

Fig. (4): Vertical profiles of mean velocity and turbulent intensity in the simulated boundary layer

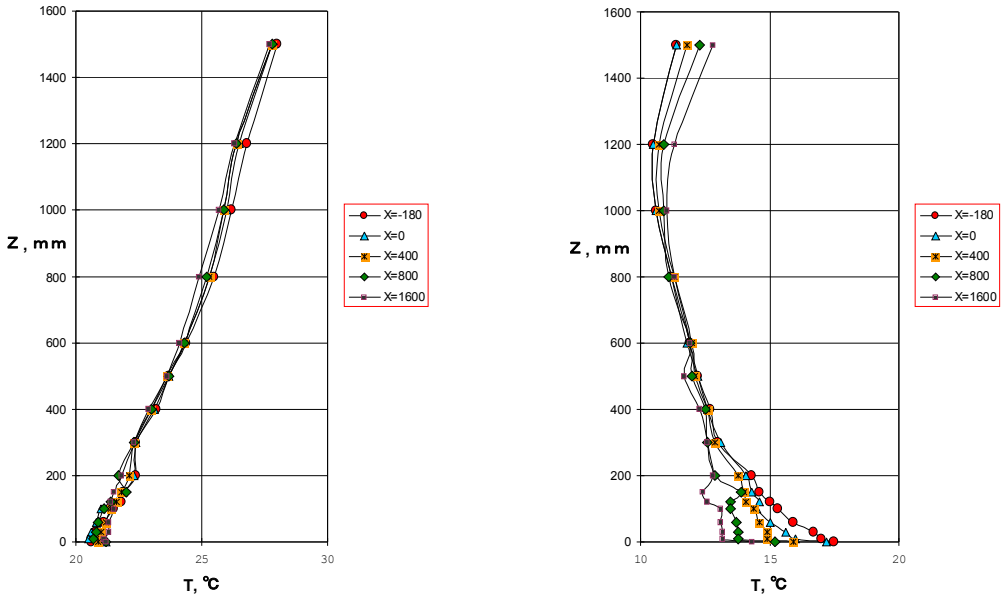

(1) stable (2) unstable

Fig. (5): Vertical profiles of temperature in the simulated boundary layer

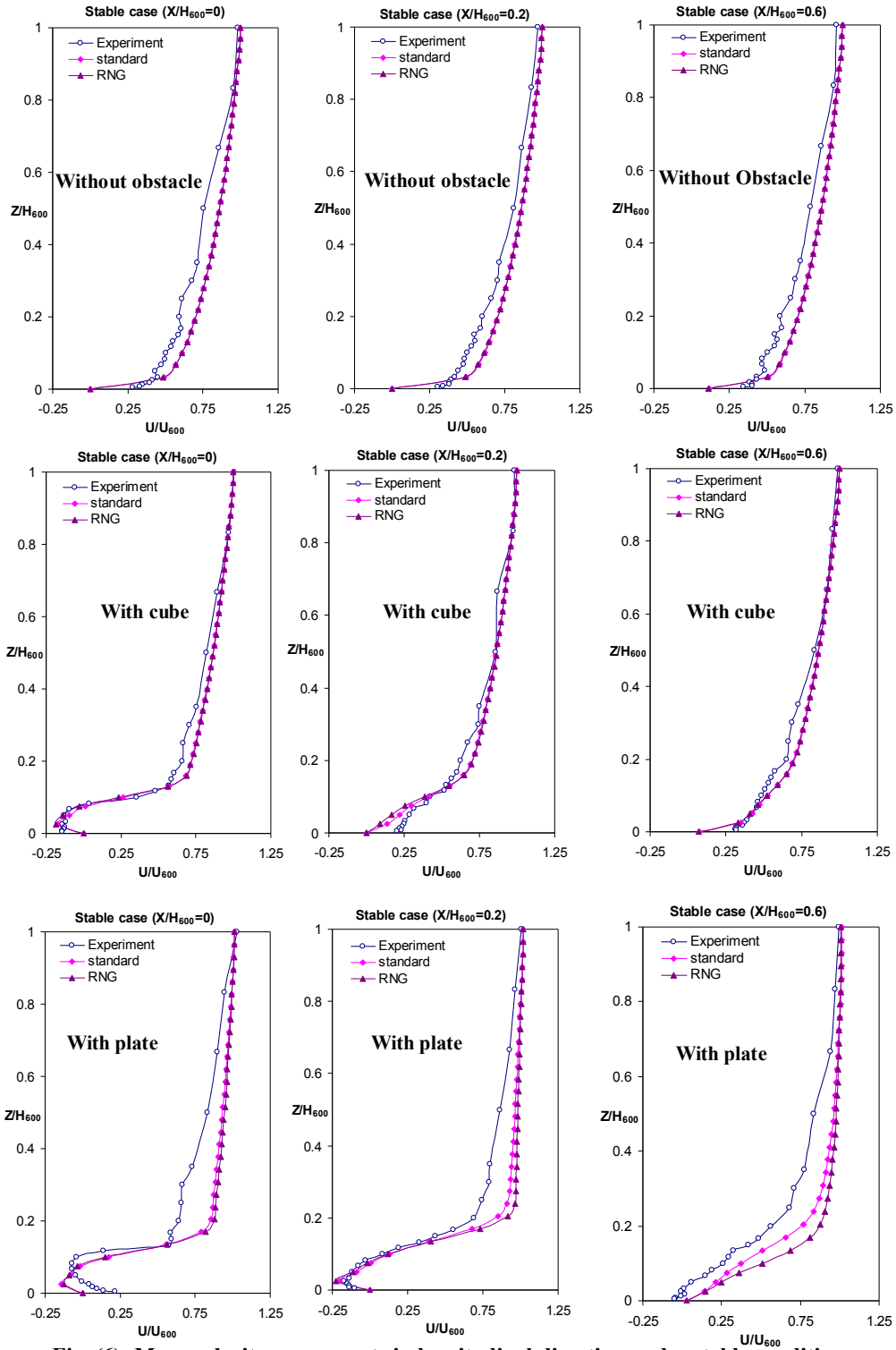

Fig. (6): Mean velocity components in longitudinal direction under stable condition

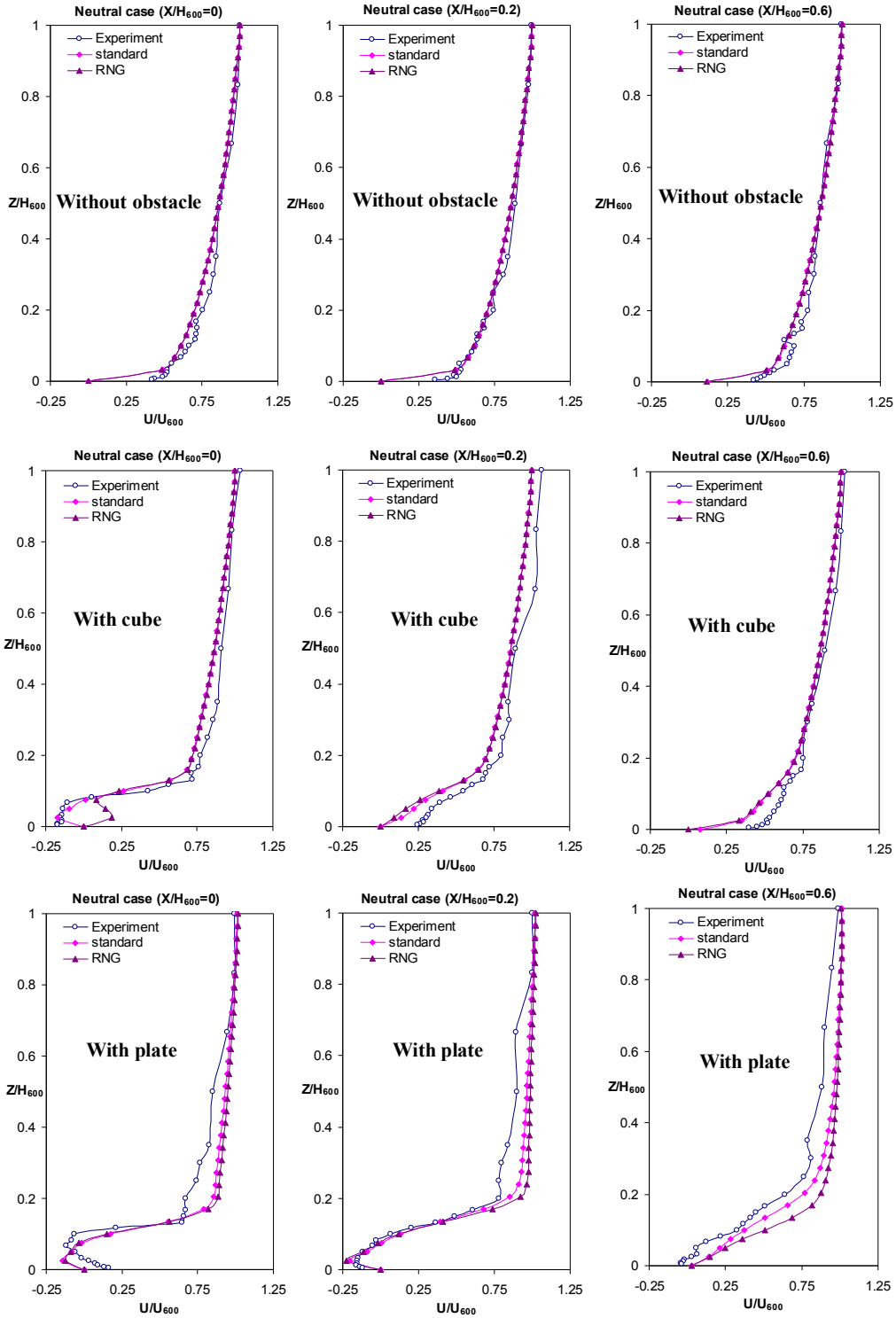

Fig. (7): Mean velocity components in longitudinal direction under neutral condition

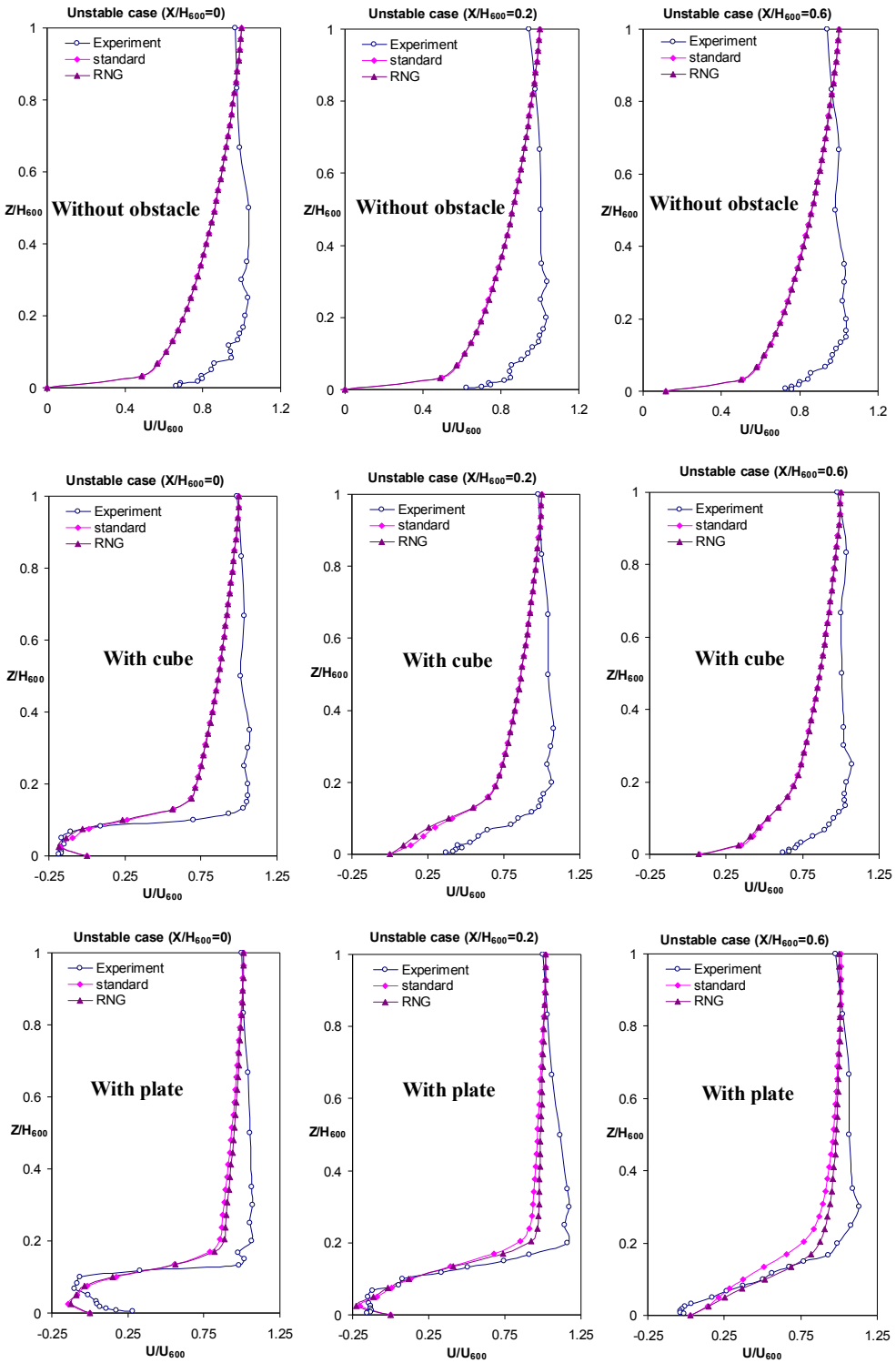

Fig. (8): Mean velocity components in longitudinal direction under unstable condition

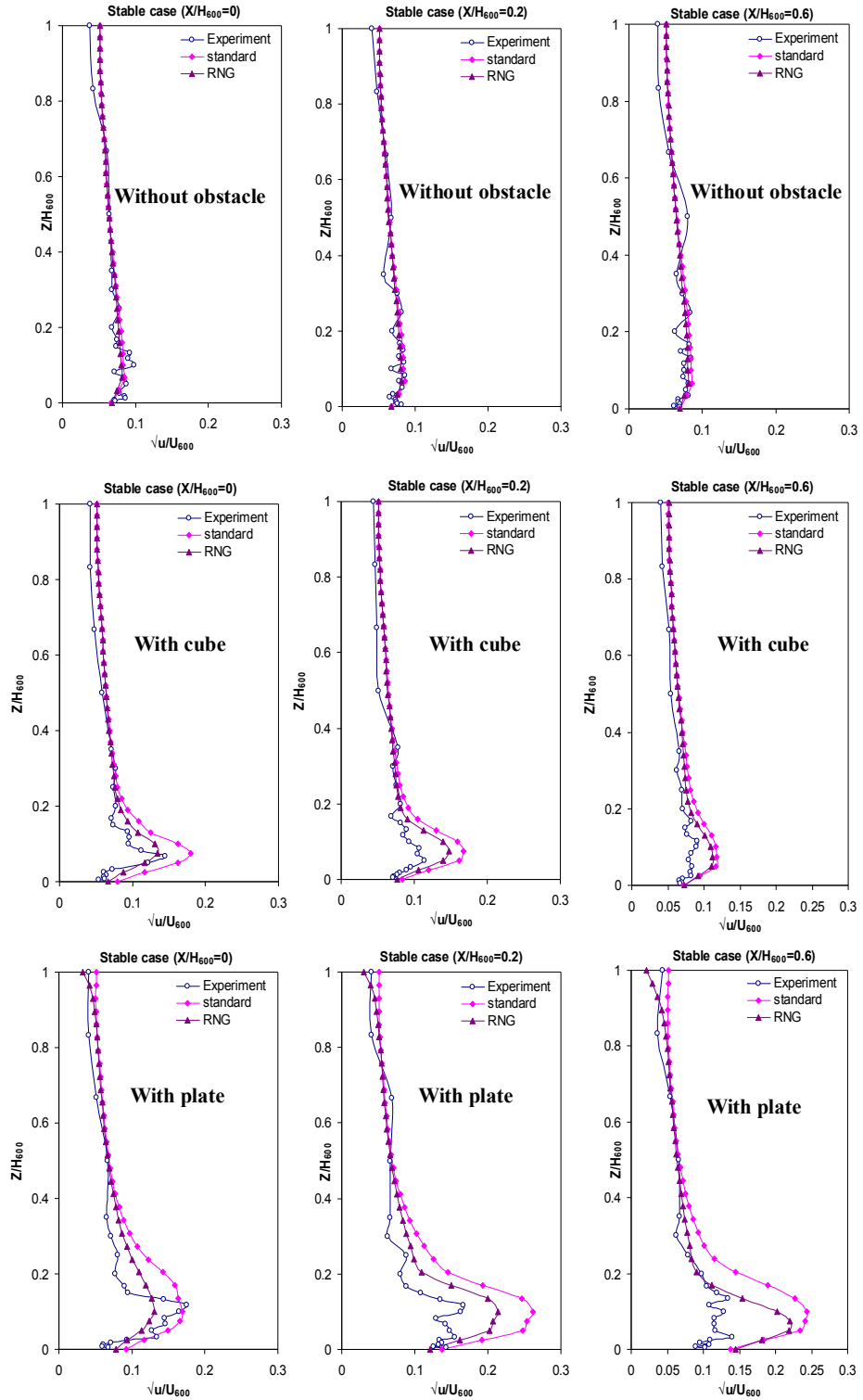

Fig. (9): Turbulence velocity components in longitudinal direction under stable condition

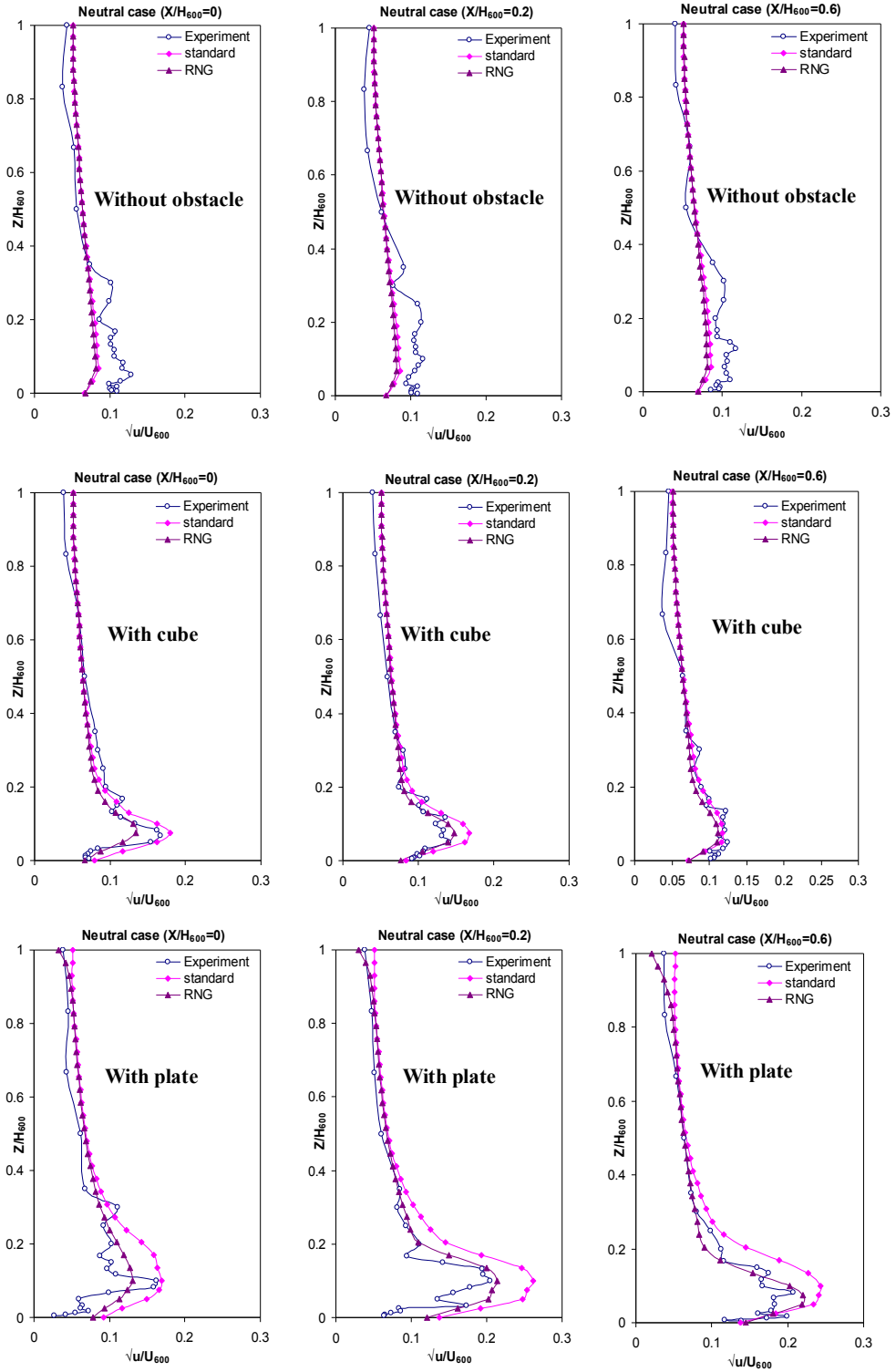

Fig. (10): Turbulence velocity components in longitudinal direction under neutral condition

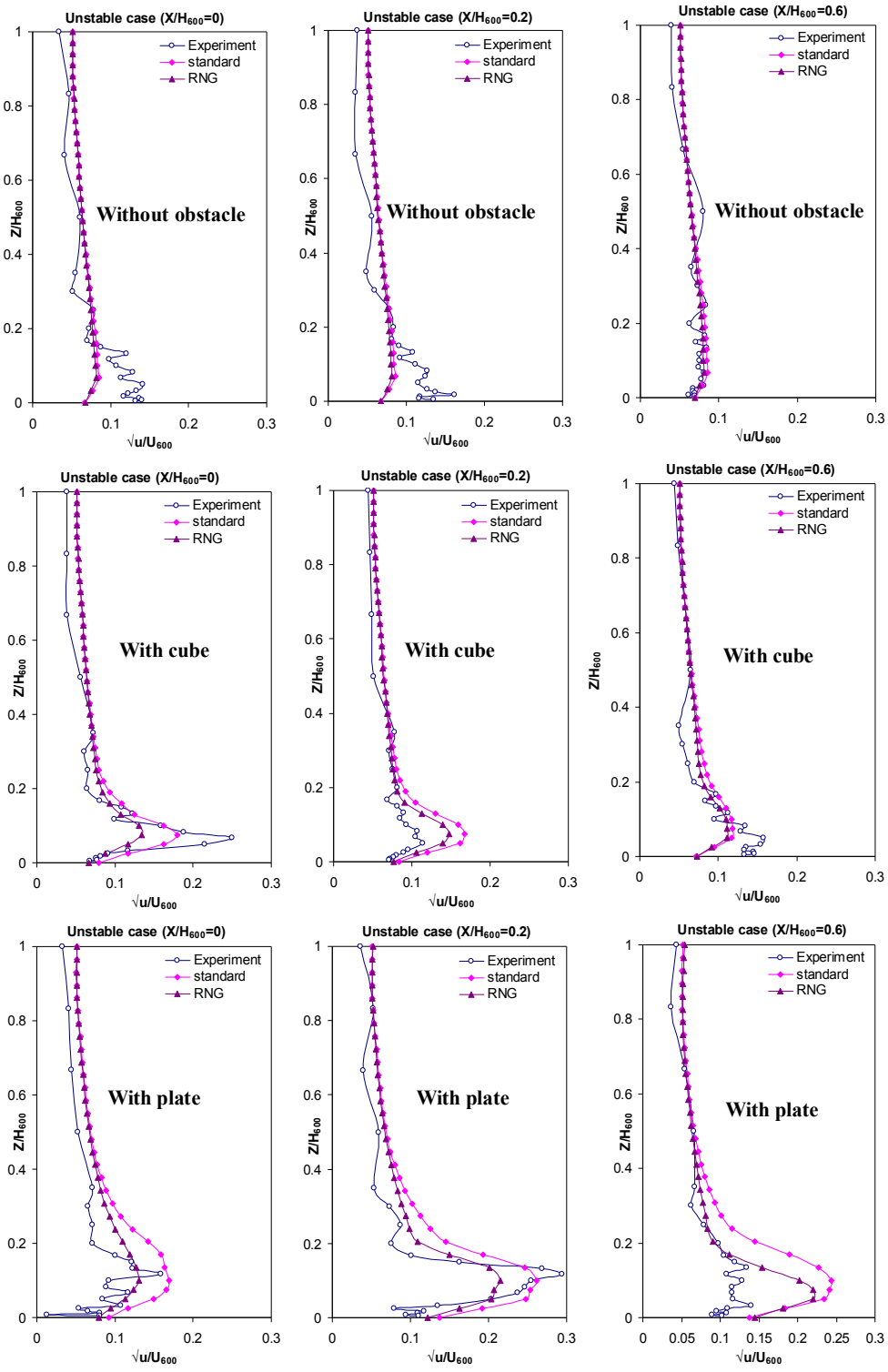

Fig. (11): Turbulence velocity components in longitudinal direction under unstable condition

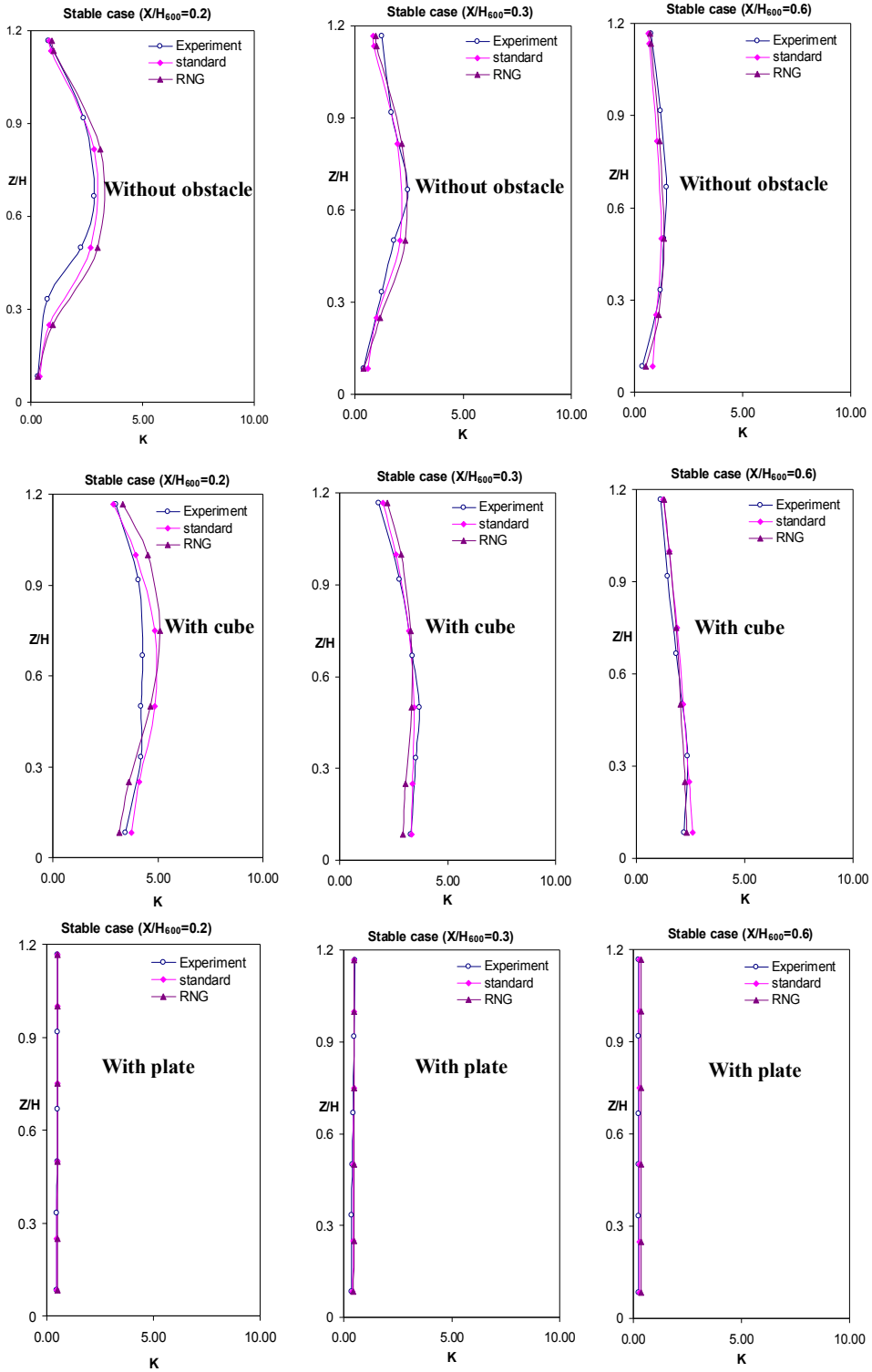

Fig. (12): Dispersion concentration, *K* with stack height, H_s/H=0.05 under stable condition

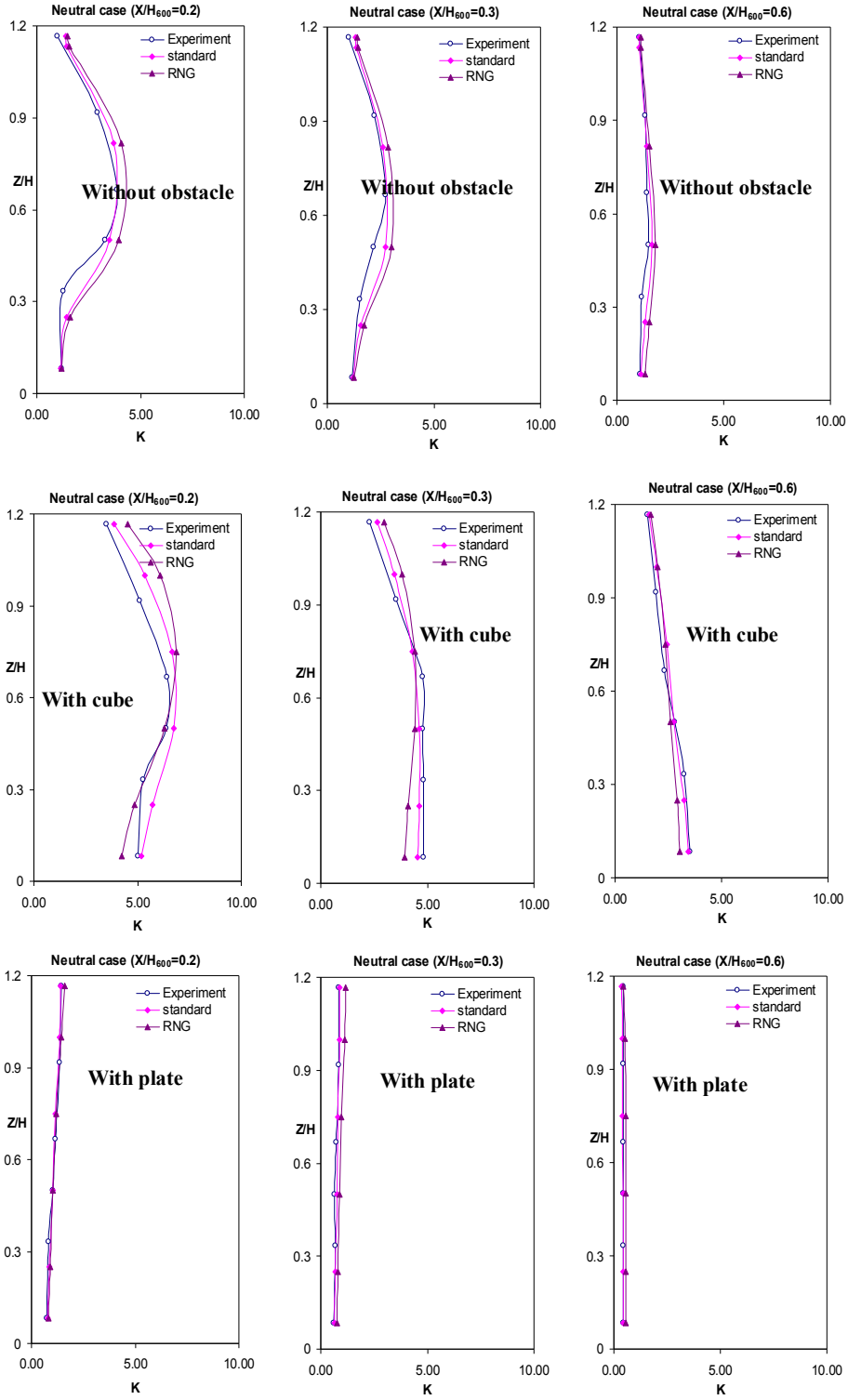

Fig. (13): Dispersion concentration, *K* with stack height, H_s/H=0.05 under neutral condition

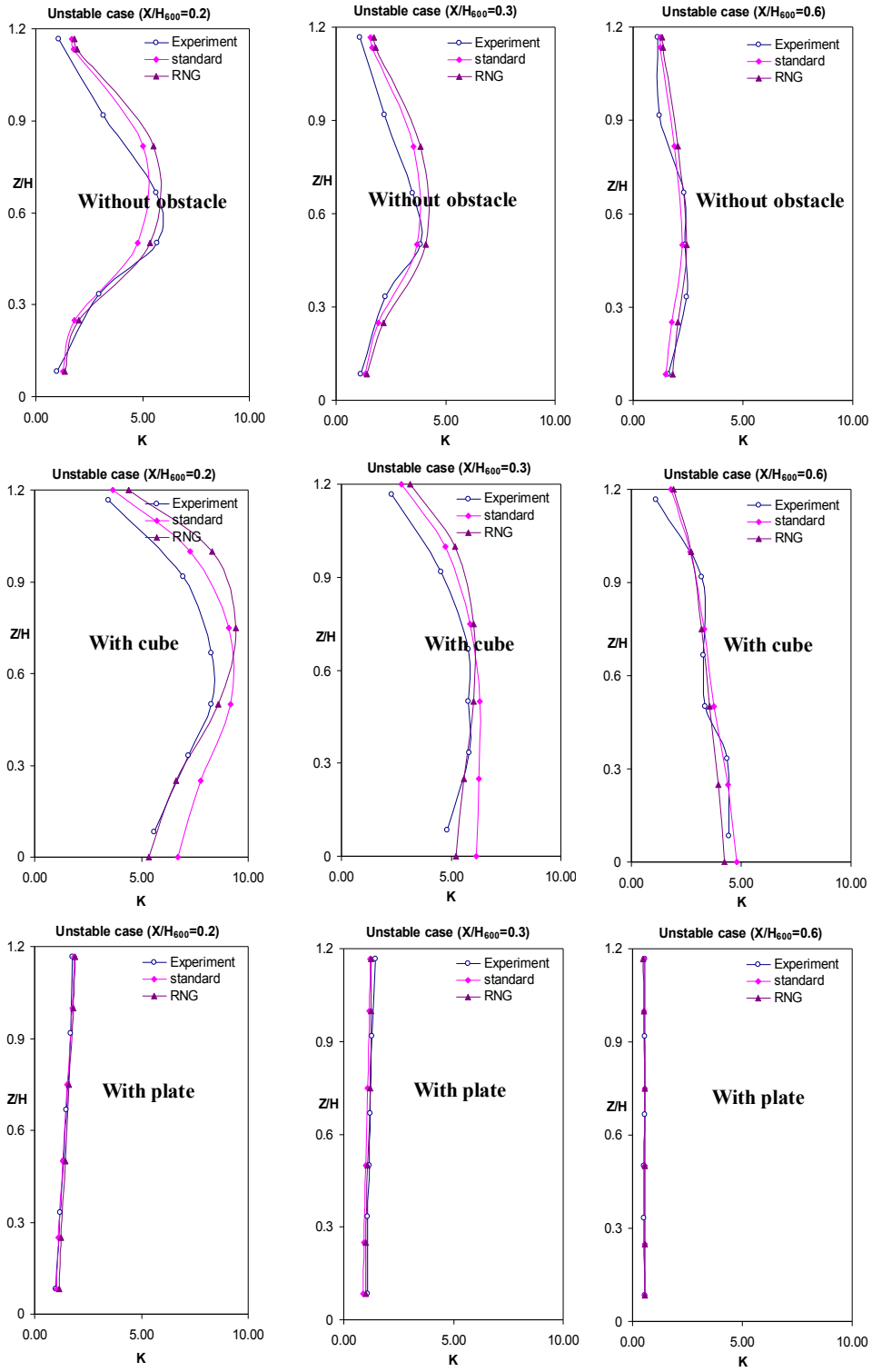

Fig. (14): Dispersion concentration, *K* with stack height, H_s/H=0.05 under unstable condition

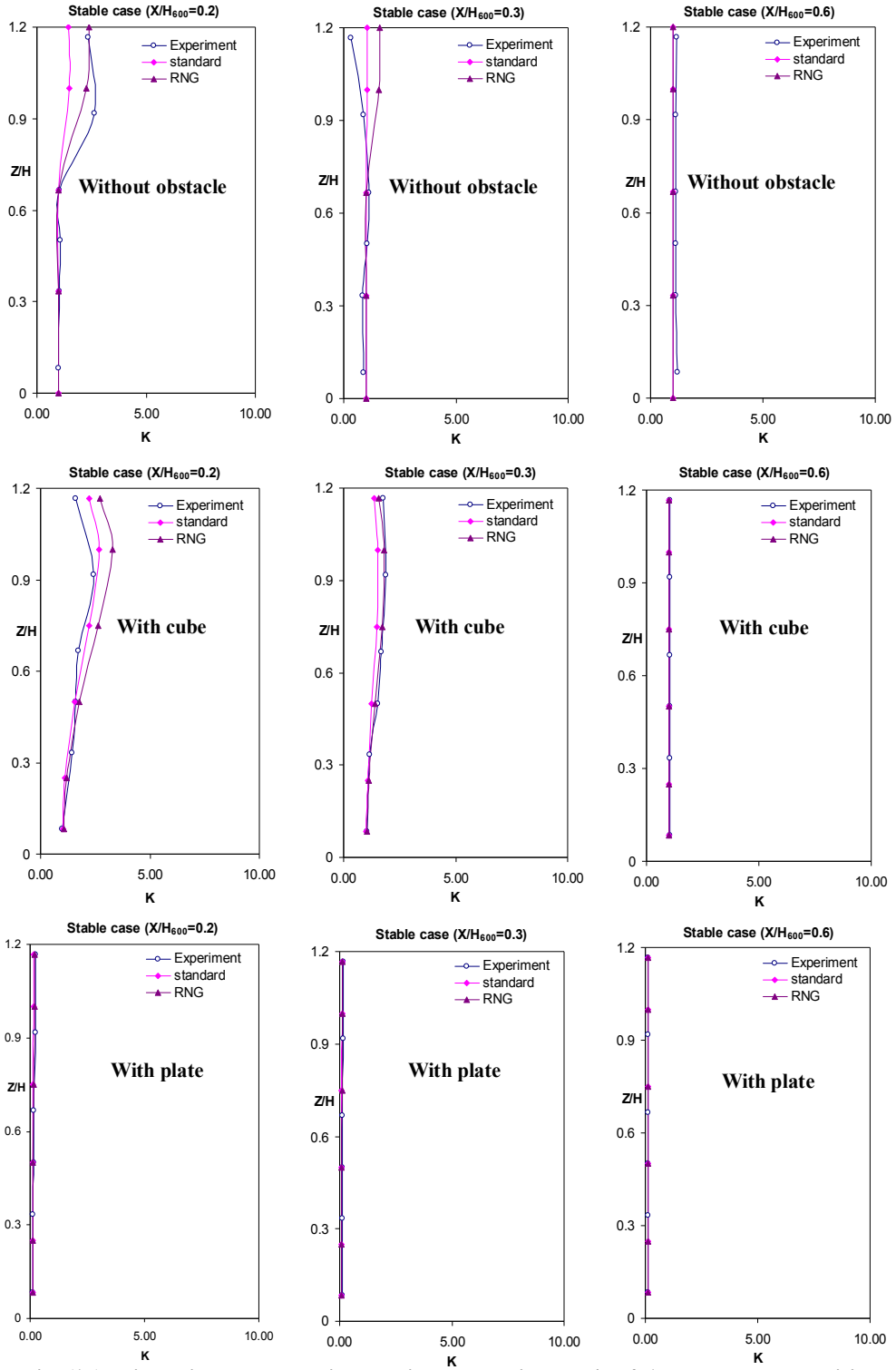

Fig. (15): Dispersion concentration, *K* with stack height, H_s/H=0.1 under stable condition

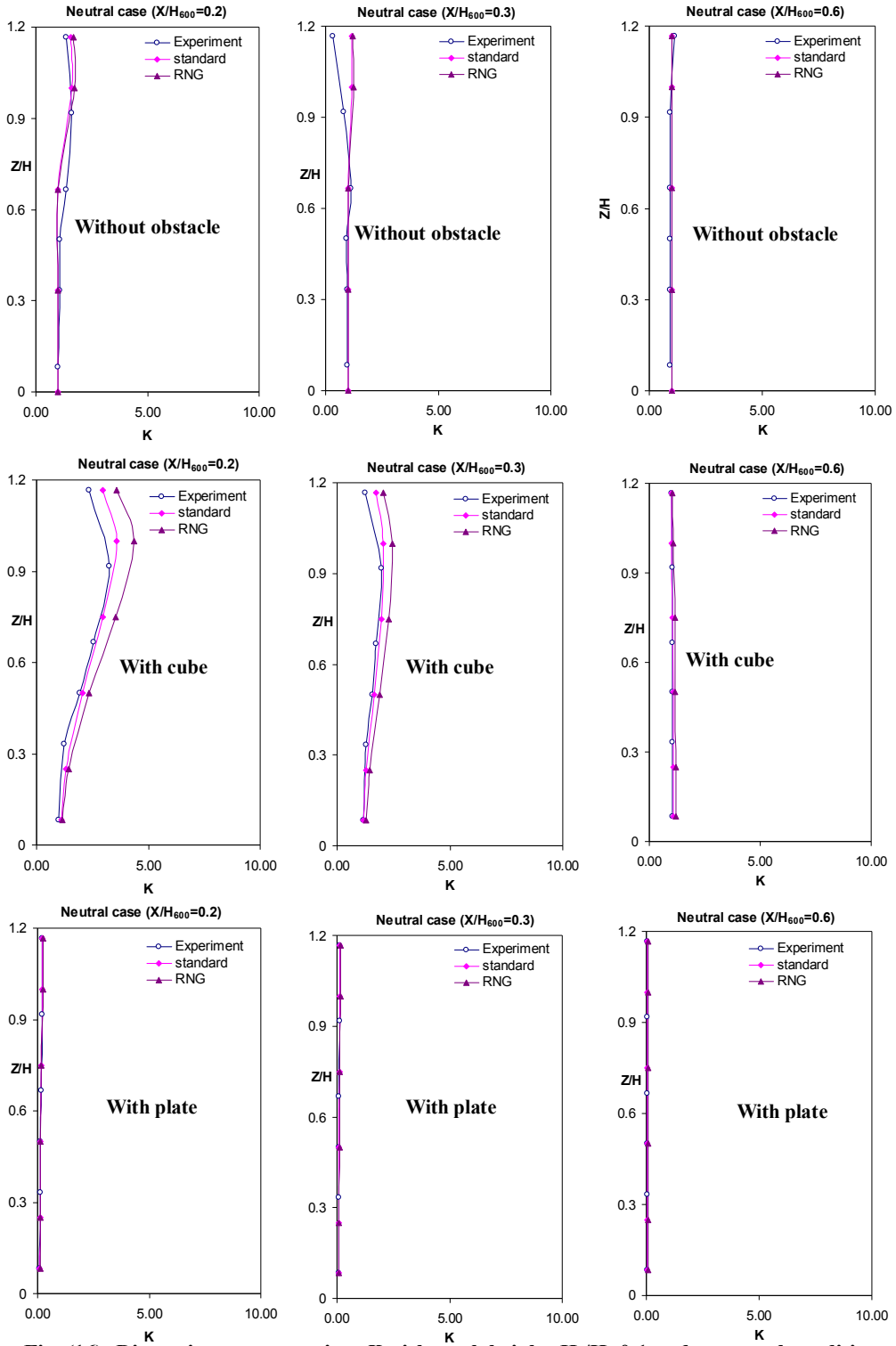

Fig. (16): Dispersion concentration, *K* with stack height, H_s/H=0.1 under neutral condition

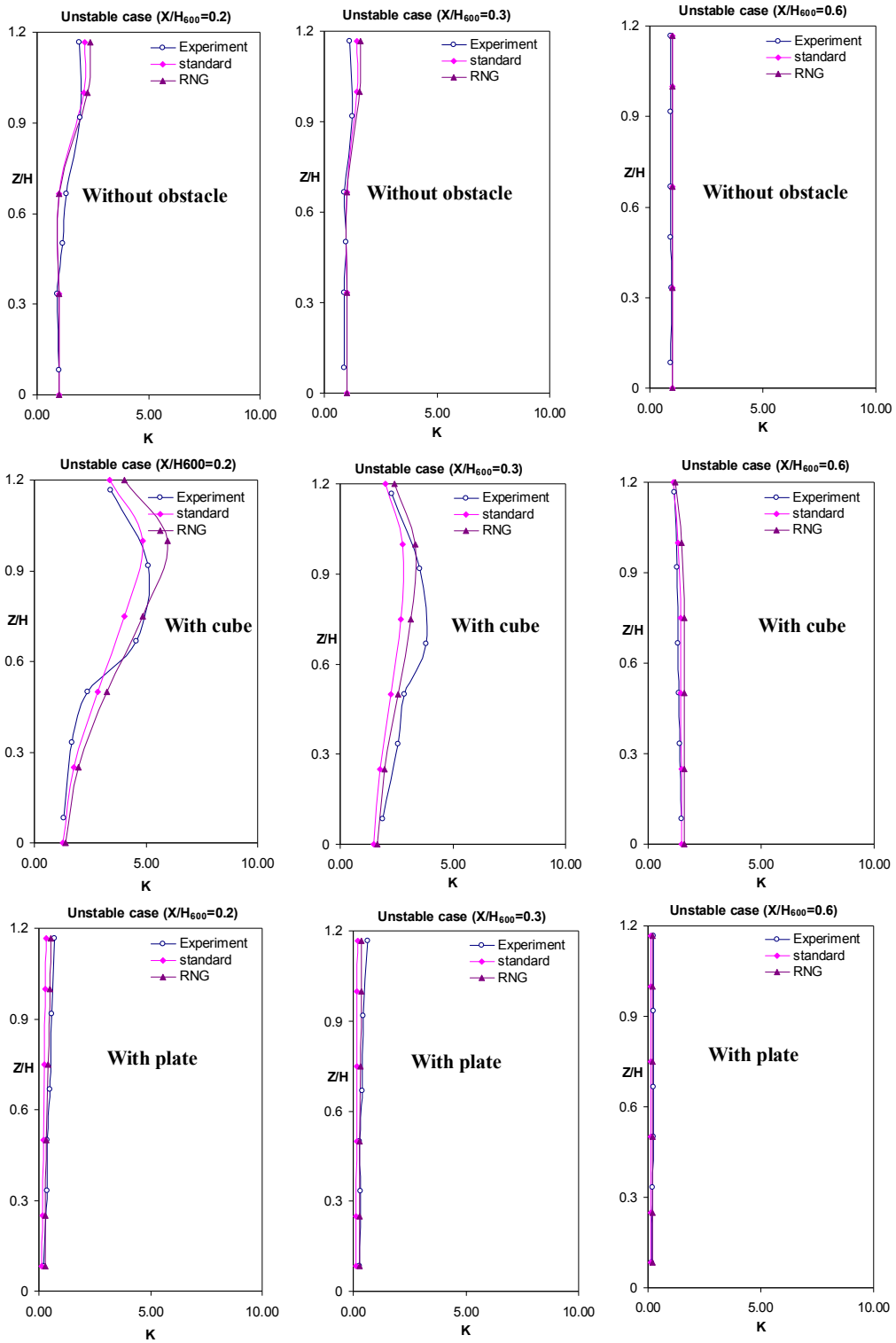

Fig. (17): Dispersion concentration, *K* with stack height, H_s/H=0.1 under unstable condition

REFERENCE:

Arya, S. P., Air Pollution Meteorology and Dispersion. Oxford University Press, Inc. Oxford, 1999.

Baik J., Kim J. and Fernando J. S. (2003) 'A CFD Model for Simulating Flow and Dispersion' J. Applied Meteorology, 42, pp. 1636-1648.

Fluent Inc., FLUENT 6.2.16 user Manual, (2005).

Halitsky J. (1963) 'Gas Diffusion Near Buildings' ASHRAE Trans., 69, pp. 464-485.

Higson H.L. and Griffiths R.F. (1994) "Concentration Measurements Around an Isolated Building: a Comparison Between wind tunnel and field data" Atmospheric Environment, Vol. 28, No. 11, pp. 1827-1836.

Huber A.H. (1989) 'Video Images of smoke dispersion in the near wake of a model building. Part II. Cross-stream dispersion', J. Wind Eng. Ind. Aerodyn., 32(1989) 263-284.

Isaacson M.S. and sandri G.V.H. (1990) 'Laboratory study of pollutant detention times in wake cavities downwind of low-rise buildings' J. Wind Eng. Ind. Aerodyn., 36, pp. 653-663.

Launder B.E. and Spalding D.E., The Numerical Computation of Turbulent Flows, Comp. Meth. Appl. Mech. Eng. 3 (1974) 269-289.

Kim J. and Baik J. (2004) 'A Numerical Study of effects of ambient wind on flow and dispersion in urban street canyons using the RNG κ-ε turbulence model, Atmospheric Environment, 38, pp. 3039-3048.

Macdonald R.W., Griffiths R.F. and Hall D.J. (1998) "A comparison of results from scaled field and wind tunnel modeling of dispersion in arrays of obstacles" Atmospheric Environment, Vol. 32, No. 22, pp. 3845-3862.

Mavroidis I. and Griffiths R.F. (2001) "Local characteristics of atmospheric dispersion within building arrays" Atmospheric Environment, Vol. 35, pp. 2941-2954.

Meroney R.N. and Yang B.T.: Wind tunnel Study on Gaseous Mixing Due to Various Stack Heights and

Injection rates above an isolated structure, CER71-72RNM-BTY16, 1971.

Meroney, R. N., Leitl, B., Rafailidis, S. and Schatzmann, M. (1999) "Wind-tunnel and numerical modeling of flow and dispersion about several building shapes," Journal of Wind Engineering and Industrial Aerodynamics, 333-345.

Mfula, A.M., Kukadia, V., Griffiths, R.F. and Hall, D.J., 2005: Wind tunnel modeling of urban building exposure to outdoor pollution. Atmospheric Environment, 39, 2737-2745.

Ogawa, Y., Griffiths R., Hoydush, W.G., A wind tunnel study of sea breeze effects. Boundary Layer Meteorology, 8, pp.141-161, 1974.

Patanker S.V. (1980) 'Numerical heat transfer and fluid flow, McGraw-hill.

Robins A.G. and Castro I.P. (1977) "A wind tunnel investigation of plume dispersion in the vicinity of surface mounted cube-II the concentration field" Atmospheric Environment, Vol. 11, pp. 299-311

Schulman and Scire, J. (1991) "The effect of stack height, exhaust speed, and wind direction on concentrations from a rooftop stack", ASHRAE Transactions, volume 97, pp 573-582 part 2.

Snyder W.H.: Downwash of Plumes in the Vicinity of Building a Wind-Tunnel

Study, NATO Advanced Research Workshop, Portugal, 1993.

Snyder W.H. and Lawson R.E.J.: Wind-Tunnel Measurement of Flow Field in the Vicinity of Building, 8th AMS Conf. on Appl. Air Poll. Meteorol., Tennessee, 1994.

Saathoff P.J., Stathopoulos and Dobrescu M. (1995) "Effect of model scale in estimating pollutant dispersion near building" Journal of Wind Engineering and Industrial Aerodynamics, Vol. 54 &55, pp. 549-559.

Wen-Whai L. and Meroney R.N. (1983) "Dispersion near a cubical model building" Part I mean concentration measurements" Journal of Wind Engineering and Industrial Aerodynamics, Vol. 12, pp. 15-33.

Wilson, D (1979) "Flow patterns over flat-roofed buildings and application to exhaust stack design", ASHRAE Transactions, 85, part 2, 284-295.

Wilson, D.J. and Lamb, B., (1994) "Dispersion of exhaust gases from roof level stacks and vents on a laboratory building", Atmospheric Environment, 28, 3099-3111.

Wilson D.J. and Britter R.E. (1982) 'Estimates of building surface concentration from nearby point sources' Atmospheric Environment, 16, pp. 2631-2646.

Yakhot V., Orszag S.A., Thangam S., Gatski T.B., and Speziale C.G. (1992) 'Development of turbulence models for shear flows by a double expansion technique, Phys. Fluids A 4 (7), pp.1510-1520.

المحاكاة العددية والدراسة التجريبية لانتشار الغازات المنبعثة من ارتفاعات مختلفة في بيئة حضرية

محمد فتحى يس

قسم هندسة التعدين والفلزات – كلية الهندسة – جامعة أسيوط

أجريت هذه الدراسة بغرض تطوير مفهوم ظاهرة انتشار الملوثات من مصادر مرتفعة حول عوائق مختلفة الارتفاعات بالنسبة للمداخن فى بيئة حضرية. وقد تم محاكاة ظروف الانتشار باستعمال نماذج ديناميكيا السوائل الحسابية . كما تم دراسة الظواهر عملياً فى نفق الانتشار الهوائى تحت ظروف حرارية مختلفة لتقييم دقة تنبؤ انتشار الغازات .

وقد أثبتت الدراسة أنه يوجد اتفاقاً بين نتائج استخدام نماذج المحاكاة العددية, وتلك التى تم الحصول عليها عملياً . كما تبين أن الحالة الغير مستقرة أعلى من الحالات المحايدة والمستقرة. ووجد أن تركيز التشتت للنموذج المكعب أعلى من نموذج الصحى.